JOURNAL OF GUIDANCE, CONTROL, AND DYNAMICS
Vol. 28, No. 3, May–June 2005

Path Planning and Open-Loop Shape Control of Modular Tensegrity Structures

Milenko Masic* and Robert E. Skelton†
University of California, San Diego, La Jolla, California 92093-0411

We characterize the planned path for a shape change in a tensegrity structure as a path from one equilibrium to another. For tensegrity structures, this means that in every desired configuration the structure has to satisfy tensegrity conditions. Required trajectories are feasible, and changes in potential energy are not required to follow these trajectories. This is a benefit over normal control paths that require strain-energy changes because such energy must be supplied by the control system. For the class of modular tensegrity structures defined, configurations that satisfy tensegrity conditions can be parameterized in terms of only a few parameters that can meaningfully be related to the overall desired shape of the structures. Equilibrium rest lengths of string elements are defined first. An open-loop rest-length control is defined by slowly varying desired geometric parameters, which causes the structure to track trajectories defined by the time-dependent geometric parameters. Examples with simulation results show different reconfiguration scenarios of tensegrity plates and class-2 tensegrity towers.

I. Introduction

A TENSEGRITY structure is a prestressable stable truss-like system. As an art form, tensegrity structures were first introduced by Snelson[1] and Fuller.[2] Unlike regular trusses, tensegrities involve string elements that are capable of transmitting load in one direction only. Therefore, the set of admissible topologies for the tensegrities is much smaller than the set of topologies that yields a finite mechanism structure. Historically, form-finding and rigidity problems have comprised the major portion of tensegrity research because of this peculiar property of tensegrity structures.[3–8]

It is fair to say that the difficulties associated with the parameterization of tensegrity geometries had a large impact on almost all areas of tensegrity research. Hence, the number of results on the shape control of tensegrities did not follow the early recognized potential of these structures. Several methods for controlling the shape of tensegrities have been proposed, from static based to dynamic based. Early proposed algorithms were mostly static methods for controlling the configuration of tensegrities. Because they could not be regarded as control algorithms in the dynamic sense, classifying them as methods for modifying shape of a tensegrity more closely describes their true character. These strategies usually require simpler actuators compared to dynamically controlled structures, and they are still considered for certain applications.[9] Some of the recently proposed concepts[10] that fall into this group include embedding bistable devices in the structures. These devices store strain energy that is used for deploying the structures.

The problem of controlling the shape of tensegrities in the dynamic sense was first addressed by Sultan, and Skelton[11,12] and Sultan et al.[13,14] Available tensegrity control results can be classified into two categories, the first[9,12,15–17] concerning tensegrity reconfigurations as tracking control problems, as opposed to the set point regulation problems[11,13,14,18,19] representing the second category. Several different dynamic models of tensegrity structures have been developed.[19–21] The nonlinear dynamic model of tensegrity structures used for the simulations shown in this paper is derived by Skelton et al.[21] and implemented in the TENSOFT software.

There are two main contributions of this paper. First, we show that the form-finding problem can be significantly simplified for the modular tensegrity structures. Because of their specific symmetry, the equilibrium conditions[22] can be broken down to a collection of smaller problems independently of the size of the original structure. The set of structure composition rules associated with modular tensegrity structures is defined. These rules represent an analytical method for the analysis of equilibrium geometries and the associated prestress for these structures. They facilitate analytical solutions of the equilibrium conditions for modular tensegrity structures of arbitrary sizes.

The second contribution of the paper is the demonstration of an open-loop control strategy based upon the static equilibria conditions. These conditions can be characterized as time dependent if the resulting motion is slow compared to the dynamics of the system. For the nonlinear system whose model and equilibria are parameterized, a sufficiently slow variation of the parameter set produces the response of the system that remains in the close proximity of the parameterized equilibrium manifold.

II. Tensegrity Equilibrium Conditions

Definition 1: The nodes ν_k, $k = 1, \ldots, n_n$ of a tensegrity structure, are the points where bars and strings of the structure connect. A nodal vector, $\boldsymbol{p}_k \in \mathbb{R}^3$, represents the position of the node ν_k. The sets of all nodes of a tensegrity structure and associated nodal vectors are denoted $\mathbb{N}$ and $\mathbb{P}$, respectively.

Definition 2: An element, $e_i = \{[\nu_k, \nu_j], z_i\}$, $k \neq j$, $i = 1, \ldots, n_e$, of a tensegrity structure is either a bar or a string that connects the two nodes ν_k and ν_j of the tensegrity. The pair $[\nu_k, \nu_j]$ is an ordered pair, and z_i identifies the element type. For the tensegrity structure with the element set $\mathbb{E}$, z_i is defined as follows:

$$z_i = \begin{cases} 1, & e_i \in \mathbb{E}_s \\ -1, & e_i \in \mathbb{E}_b \end{cases} \tag{1}$$

where $\mathbb{E}_s \in \mathbb{E}$ and $\mathbb{E}_b \in \mathbb{E}$ are the subsets of the string and bar elements of the tensegrity structure.

Definition 3: An element vector, $\boldsymbol{g}_i \in \mathbb{R}^3$, is a vector along the length of an element $e_i = \{[\nu_k, \nu_j], z_i\}$. It emanates from the first node ν_k and terminates at the second node ν_j of the element, that is,

$$\boldsymbol{g}_i = \boldsymbol{p}_j - \boldsymbol{p}_k$$

Received 5 December 2003; revision received 8 June 2004; accepted for publication 8 June 2004.

*Postdoctoral Researcher, Mechanical and Aerospace Engineering Department, Structural Systems and Control Lab, 9500 Gilman Drive; mmasic@mae.ucsd.edu.

†Professor, Mechanical and Aerospace Engineering Department, Structural Systems and Control Lab, 9500 Gilman Drive.

It is obvious that magnitude of an element vector $\boldsymbol{g}_i$ is equal to its length $\|\boldsymbol{g}_i\|$, which is denoted by l_i.

Definition 4: The element force vector $\boldsymbol{f}_{ji} \in \mathbb{R}^3$ represents the contribution of the internal force of the element e_i to the balance of the forces at the node ν_j, and it can be written as

$$\boldsymbol{f}_{ji} = c_{ji}\lambda_i \boldsymbol{g}_i, \qquad f_i = \lambda_i \|\boldsymbol{g}_i\| = \lambda_i l_i \tag{2}$$

where element force density λ_i is a scalar.

Obviously, scalars c_{ji} in Eq. (2), which are defined as the typical elements of the matrix $C(\mathbb{E}) \in \mathbb{R}^{n_n \times n_e}$, take on one of the following values: $c_{ji} = \pm 1$ or $c_{ji} = 0$.

Let $\mathbb{R}^n_m$ denote the vector space of vectors $\boldsymbol{x}$ that have the following structure:

$$\boldsymbol{x} \in \mathbb{R}^n_m \Rightarrow \boldsymbol{x}^T = [\boldsymbol{x}_1 \quad \boldsymbol{x}_2 \quad \cdot \quad \boldsymbol{x}_n]^T, \qquad \boldsymbol{x}_i \in \mathbb{R}^m, \qquad \mathbb{R}^m = \mathbb{R}^m_1 \tag{3}$$

Nodal vector $\boldsymbol{p} \in \mathbb{R}^{n_n}_3$, element vector $\boldsymbol{g}(\mathbb{E}, \mathbb{P}) \in \mathbb{R}^{n_e}_3$, force density vector $\boldsymbol{\lambda} \in \mathbb{R}^{n_e}$, and vector $\boldsymbol{z} \in \mathbb{R}^{n_e}$ are formed by collecting all of the nodal vectors $\boldsymbol{p}_i$, element vectors $\boldsymbol{g}_i$, force densities λ_i, and the individual element type identifiers

$$\boldsymbol{p} = \begin{bmatrix} \boldsymbol{p}_1 \\ \boldsymbol{p}_2 \\ \cdot \\ \boldsymbol{p}_{n_n} \end{bmatrix}, \qquad \boldsymbol{g} = \begin{bmatrix} \boldsymbol{g}_1 \\ \boldsymbol{g}_2 \\ \cdot \\ \boldsymbol{g}_{n_e} \end{bmatrix}$$

$$\boldsymbol{\lambda} = \begin{bmatrix} \lambda_1 \\ \lambda_2 \\ \cdot \\ \lambda_{n_e} \end{bmatrix}, \qquad \boldsymbol{z} = \begin{bmatrix} z_1 \\ z_2 \\ \cdot \\ z_{n_e} \end{bmatrix} \tag{4}$$

Let the member-node incidence matrix of the oriented graph associated with $\mathbb{E}$ be denoted $M(\mathbb{E}) \in \mathbb{R}^{n_e \times n_n}$, and let $\boldsymbol{M} \in \mathbb{R}^{3n_e \times 3n_n}$ be defined as $\boldsymbol{M} = M \otimes I_3$. The typical element m_{ij} of the matrix M is $m_{ij} = 1$ or $m_{ij} - 1$ if the element e_i terminates at or emanates from the node ν_j; otherwise, $m_{ij} = 0$. Let the n_s string elements in $\mathbb{E}_s$ be numbered first. Then, vector $\boldsymbol{g}$ and matrix $\boldsymbol{M}$ can be partitioned as follows:

$$\boldsymbol{g} = \begin{bmatrix} \boldsymbol{g}_s \\ \boldsymbol{g}_b \end{bmatrix} = \boldsymbol{M}\boldsymbol{p}, \qquad \boldsymbol{M} = \begin{bmatrix} \boldsymbol{S}^T \\ \boldsymbol{B}^T \end{bmatrix}, \qquad \boldsymbol{S} \in \mathbb{R}^{3n_n \times 3n_s}$$

One can show that equilibrium conditions for the prestressed structure with strings under tension can be written as

$$\boldsymbol{C}\tilde{\boldsymbol{g}}\boldsymbol{\lambda} = 0, \qquad \|\boldsymbol{\lambda}\| > 0, \qquad \underline{\lambda}_i \geq 0, \qquad e_i \in \mathbb{E}_s \tag{5}$$

$$\boldsymbol{C} = [-\boldsymbol{S} \quad \boldsymbol{B}], \qquad \boldsymbol{g} = \boldsymbol{M}\boldsymbol{p} = \begin{bmatrix} \boldsymbol{S}^T \\ \boldsymbol{B}^T \end{bmatrix} \boldsymbol{p} \tag{6}$$

if the linear operator ~ acting on the vector $\boldsymbol{x} \in \mathbb{R}^n_m$ is defined as follows:

$$\tilde{\boldsymbol{x}} := \mathrm{blockdiag}\{\boldsymbol{x}_1 \ldots, \boldsymbol{x}_i, \ldots \boldsymbol{x}_n\} \in \mathbb{R}^{mn \times n}, \qquad \boldsymbol{x}_i \in \mathbb{R}^m$$

Let the tensegrity structure Γ, defined by the triple $\Gamma = \{E, \mathbb{P}, \boldsymbol{\lambda}\}$, admit element and nodal symmetry $I(\boldsymbol{x})$ (Ref. 22), so that all of its elements and nodes can be grouped, respectively, in n_{ec} and n_{nc} element and node equivalence classes. Then, the full vector of force densities $\boldsymbol{\lambda}$ can be expressed as a linear mapping from the reduced set of the independent force density variables $\underline{\boldsymbol{\lambda}} \in R^{n_{\mathrm{ec}}}$, by defining matrix $Q \in R^{n_e \times n_{\mathrm{ec}}}$. Furthermore, the size of the problem can be reduced by keeping only the set of independent equations in Eq. (5). This can be accomplished by multiplying the equality in Eq. (5) from the left with a sparse matrix $\boldsymbol{D} \in \mathbb{R}^{3n_{\mathrm{nc}} \times 3n_n}$. The structure of the matrices Q and $\boldsymbol{D}$ corresponding to the symmetric problem is given by Masic et al.[22] and Masic.[23] If a change of geometric variables is defined so that $\boldsymbol{p} = \boldsymbol{p}(\boldsymbol{\alpha}, \boldsymbol{\beta}, \boldsymbol{\gamma}, \ldots)$ and the shape constraints in the form $\varphi(\boldsymbol{\alpha}, \boldsymbol{\beta}, \boldsymbol{\gamma} \ldots) = 0$ are included in the problem, the symmetric tensegrity form-finding problem becomes as follows:

Given data, $\boldsymbol{D}, \boldsymbol{S}, \boldsymbol{B}, Q, \mathcal{R}, \mathbb{E}_s$, find $\underline{\boldsymbol{\lambda}}, \boldsymbol{\alpha}, \boldsymbol{\beta}, \boldsymbol{\gamma}, \ldots$, such that

$$\boldsymbol{D}\boldsymbol{C}\tilde{\boldsymbol{g}}Q\underline{\boldsymbol{\lambda}} = 0, \qquad \boldsymbol{C} = [-\boldsymbol{S} \quad \boldsymbol{B}], \qquad \underline{\boldsymbol{p}} = \underline{\boldsymbol{p}}(\boldsymbol{\alpha}, \boldsymbol{\beta}, \boldsymbol{\gamma}, \ldots)$$

$$\boldsymbol{p} = \mathcal{R}\underline{\boldsymbol{p}}, \qquad \boldsymbol{g} = \boldsymbol{M}\boldsymbol{p} = \begin{bmatrix} \boldsymbol{S}^T \\ \boldsymbol{B}^T \end{bmatrix} \boldsymbol{p}, \qquad \varphi(\boldsymbol{\alpha}, \boldsymbol{\beta}, \boldsymbol{\gamma}, \ldots) = 0$$

$$\|Q\underline{\boldsymbol{\lambda}}\| > 0, \qquad \underline{\lambda}_i \geq 0, \qquad e_i \in \mathbb{E}_s \tag{7}$$

A more detailed explanation of tensegrity equilibrium equations (5) and (6) and their form for symmetric structures [Eqs. (7)] can be found in the literature.[22,23]

III. Composition of Tensegrity Structures

The equilibrium equation (5) can exhibit a particular structured form under certain shape constraints. The structure of these equations can be exploited to simplify their solution. The planar tensegrity of Fig. 1 is given as the example that supports these claims and motivates the analysis that follows. The sparsity pattern of the matrix $\boldsymbol{C}\tilde{\boldsymbol{g}}$ of this structure indicates that the set of equilibrium equations represents the combination of two almost decoupled linear equations in force density variables $\boldsymbol{\lambda}$. Equation (5) can be cast in the similar structured form for a large class of tensegrity structures. This highly structured problem can be further decomposed into several decoupled blocks of equations, each of which represents the equilibrium conditions for a smaller substructure. Several definitions and rules will provide the method for composition and decomposition of tensegrity structures to simplify their equilibrium analysis.

Definition 5: Node ν_r of the structure Γ is said to be attached to element $e_i = \{[\nu_j, \nu_k], z_i\}$ if element e_i is replaced in the structure

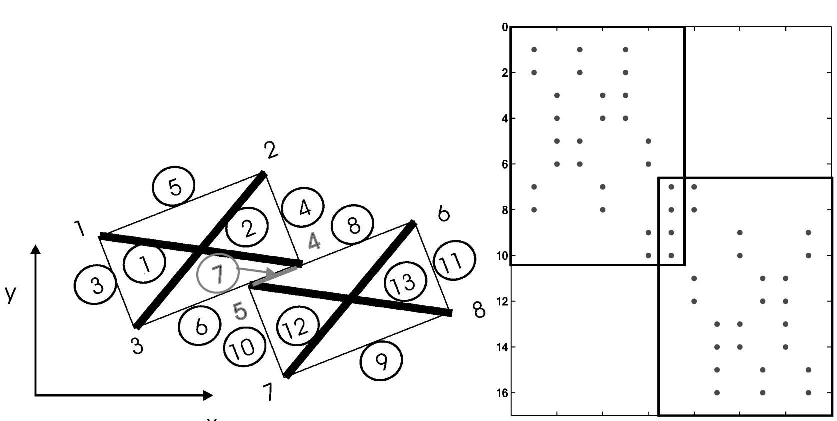

Fig. 1 Sparsity pattern of equilibrium equations for a composition of two tensegrity structures.

definition with elements $e_q = \{[\nu_j, \nu_r], z_i\}$ and $e_s = \{[\nu_r, \nu_k], z_i\}$. This will formally be written as $[e_q, e_s] = \nu_r @ e_i$.

Definition 6: Node ν_r of structure Γ is said to be attached to node ν_j if node ν_r is replaced by node ν_j in the definition of all elements incident with node ν_r. This will formally be written as $\nu_r \leftarrow \nu_j$.

The node attachment $\nu_r \leftarrow \nu_j$ should not be confused with the node placement $\boldsymbol{p}_r = \boldsymbol{p}_j$. Although the former operation removes node ν_r from the set $\mathbb{N}$, and consequently $\boldsymbol{p}_r$ from the set $\mathbb{P}$, the latter operation only place node ν_r at the position of the node ν_j, so that both these overlapping nodes continue to exist.

Definition 7: Superposition of two overlapping elements $e_i = \{[\nu_j, \nu_k], z_i\}$ and $e_q = \{[\nu_j, \nu_k], z_i\}$ or $e_q = \{[\nu_k, \nu_j], z_i\}$ of structure Γ is the operation in which element e_q is deleted from the set $\mathbb{E}$. This will formally be written as $e_q \leftarrow e_i$.

The following theorem concerns the composition of equilibrium structures and the main property associated with the result of this composition.

Theorem 1: Let the tensegrity structure $\Gamma = \{\mathbb{E}, \mathbb{P}, \boldsymbol{\lambda}\}$ be defined from the two equilibrium tensegrity structures $\Gamma_1 = \{\mathbb{E}^1, \mathbb{P}^1, \boldsymbol{\lambda}^1\}$ and $\Gamma_2 = \{\mathbb{E}^2, \mathbb{P}^2, \boldsymbol{\lambda}^2\}$ by attaching some nodes of structure Γ_1 to elements or nodes of structure Γ_2 and by attaching some nodes of structure Γ_2 to elements or nodes of structure Γ_1, so that all of the following conditions are satisfied:

1) If node ν_r is attached to node ν_j, then the nodal vectors satisfy $\boldsymbol{p}_r = \boldsymbol{p}_j$.

2) If node ν_r is attached to element $e_i = \{[\nu_j, \nu_k], z_i\}$, so that $[e_q, e_s] = \nu_r @ e_i$, then the nodal vector $\boldsymbol{p}_r$ satisfies

$$\boldsymbol{p}_r = \boldsymbol{p}_j + a(\boldsymbol{p}_k - \boldsymbol{p}_j) \qquad \text{for} \qquad 0 < a < 1 \tag{8}$$

and force densities λ_p and λ_q of elements e_p and e_q satisfy

$$\lambda_h = \lambda_i \|\boldsymbol{g}_i\|_2 / \|\boldsymbol{g}_h\|_2 = f_i / l_h, \qquad h = q, s \tag{9}$$

3) If overlapping elements e_i with force density λ_i and e_j with force density λ_j are generated and replaced by their superposition $e_j \leftarrow e_i$, the force density of the remaining element is $\lambda_j + \lambda_i$, that is,

$$\lambda_i \leftarrow \lambda_j + \lambda_i$$

Then, structure Γ is an equilibrium structure.

Structure Γ of Theorem 1 is said to be the composition of the two component structures Γ_1 and Γ_2.

Proof: The equilibrium conditions of structures $\Gamma_1 = \{\mathbb{E}^1, \mathbb{P}^1, \boldsymbol{\lambda}^1\}$ and $\Gamma_2 = \{\mathbb{E}^2, \mathbb{P}^2, \boldsymbol{\lambda}^2\}$ are defined as follows:

$$\begin{bmatrix} \boldsymbol{C}(\mathbb{E}^1) & 0 \\ 0 & \boldsymbol{C}(\mathbb{E}^2) \end{bmatrix} \begin{bmatrix} \tilde{\boldsymbol{g}}^1 & 0 \\ 0 & \tilde{\boldsymbol{g}}^2 \end{bmatrix} \begin{bmatrix} \boldsymbol{\lambda}^1 \\ \boldsymbol{\lambda}^2 \end{bmatrix} = 0 \tag{10}$$

where

$$\boldsymbol{g}^1 = \boldsymbol{g}(\mathbb{E}^1, \mathbb{P}^1), \qquad \boldsymbol{g}^2 = \boldsymbol{g}(\mathbb{E}^2, \mathbb{P}^2) \tag{11}$$

Consider first the case where nodes of Γ_2 are attached to nodes of Γ_1. Without loss of generality, assume that only node ν_r of Γ_2 is attached to the node ν_j of Γ_1. Although the definitions of elements incident with the node ν_r have changed, the vector of element vectors of the new structure $\Gamma = \{\mathbb{E}, \mathbb{P}, \boldsymbol{\lambda}\}$ remains the same as the vector of the disjoint structures, that is,

$$\boldsymbol{g} = \begin{bmatrix} \boldsymbol{g}^1 \\ \boldsymbol{g}^2 \end{bmatrix}$$

Let the connectivity matrices be partitioned as follows:

$$\boldsymbol{C}^T(\mathbb{E}^1) = \begin{bmatrix} \boldsymbol{C}^T_{1_{j-}} & \boldsymbol{C}^T_{1_j} & \boldsymbol{C}^T_{i_{j+}} \end{bmatrix}, \qquad \boldsymbol{C}^T(\mathbb{E}^2) = \begin{bmatrix} \boldsymbol{C}^T_{2_{r-}} & \boldsymbol{C}^T_{2_r} & \boldsymbol{C}^T_{2_{r+}} \end{bmatrix} \tag{12}$$

where $\boldsymbol{C}_{1_j}$ and $\boldsymbol{C}_{2_r}$ denote the rows of the matrices corresponding to the nodes ν_j and ν_r, respectively. The connectivity matrix $C(\mathbb{E})$ and the equilibrium conditions for the structure Γ have the following form:

$$\left[\begin{array}{c|c} & \\ \boldsymbol{C}_{1_{j-}} & \\ \boldsymbol{C}_j & \boldsymbol{C}_{2_r} \\ \boldsymbol{C}_{1_{j+}} & \\ \hline 0 & \boldsymbol{C}_{2_{r-}} \\ 0 & \boldsymbol{C}_{2_{r+}} \end{array}\right] \begin{bmatrix} \tilde{\boldsymbol{g}}^1 & 0 \\ 0 & \tilde{\boldsymbol{g}}^2 \end{bmatrix} \begin{bmatrix} \boldsymbol{\lambda}^1 \\ \boldsymbol{\lambda}^2 \end{bmatrix} = 0$$

Compared to the disjoint structures, the new equilibrium conditions are altered only at the node ν_j, and they have the following form:

$$\boldsymbol{C}_j \boldsymbol{g}^1 \boldsymbol{\lambda}^1 + \boldsymbol{C}_r \boldsymbol{g}^2 \boldsymbol{\lambda}^2 = 0 \tag{13}$$

From Eq. (10),

$$\boldsymbol{C}_j \boldsymbol{g}^1 \boldsymbol{\lambda}^1 = 0, \qquad \boldsymbol{C}_r \boldsymbol{g}^2 \boldsymbol{\lambda}^2 = 0$$

which shows that Eq. (13) holds true in the new connected configuration. This proves that attaching nodes to nodes does not violate the equilibrium if condition 1 is satisfied.

Consider now the second case, where nodes of Γ_2 are attached to elements of Γ_1. Without loss of generality, assume that only node ν_r of Γ_2 is attached to the string element $e_i = \{[\nu_j, \nu_k], z_i\}$ of Γ_1, so that $[e_q, e_s] = \nu_r @ e_i$, and $e_q = \{[\nu_j, \nu_r], z_i\}$, $e_s = \{[\nu_r, \nu_k], z_i\}$. Let $C(\mathbb{E}^1)$, $\boldsymbol{g}(\mathbb{E}^1, \mathbb{P}^1)$, and $\boldsymbol{\lambda}^1$ be partitioned as follows:

$$\boldsymbol{C}(\mathbb{E}^1) = [\boldsymbol{C}^{1_{i-}} \quad \boldsymbol{C}^{1_i} \quad \boldsymbol{C}^{1_{i+}}], \qquad \boldsymbol{g}^1 = \boldsymbol{g}(\mathbb{E}^1, \mathbb{P}^1) = \begin{bmatrix} \boldsymbol{g}^1_{i-} \\ \boldsymbol{g}^1_i \\ \boldsymbol{g}^1_{i+} \end{bmatrix}$$

$$\boldsymbol{\lambda}^1 = \begin{bmatrix} \boldsymbol{\lambda}^1_{i-} \\ \lambda^1_i \\ \boldsymbol{\lambda}^1_{i+} \end{bmatrix}$$

After attaching the node ν_r to the element e_i, the new equilibrium conditions must be defined. Note that the definition of the elements of $\mathbb{E}^2$ is not affected by attaching the node ν_r to the element e_i, so that $\boldsymbol{C}(\mathbb{E}^2)$, $\boldsymbol{g}^2$, and $\boldsymbol{\lambda}^2$ do not need to be redefined. To account for the substitution of the element e_i with the two new elements e_q, e_s, we define the new element vector

$$\boldsymbol{g}^{1'} = \begin{bmatrix} \boldsymbol{g}^1_{i-} \\ \boldsymbol{g}_q \\ \boldsymbol{g}_s \\ \boldsymbol{g}^1_{i+} \end{bmatrix}$$

and redefine connectivity matrix $C(\mathbb{E})$ of the new structure. This is accomplished by substituting the column corresponding to the element e_i of the connectivity matrix in Eq. (10), with the two columns that correspond to the newly formed elements e_q and e_s. With this, the equilibrium conditions of the new structure have the following form:

$$\left[\begin{array}{c|cc|c|c} & 0 & 0 & & \\ & I & 0 & \leftarrow \nu_j & \\ \boldsymbol{C}^{1_{i-}} & 0 & 0 & \boldsymbol{C}^{1_{i+}} & 0 \\ & 0 & -I & \leftarrow \nu_k & \\ & 0 & 0 & & \\ \hline & 0 & 0 & & \boldsymbol{C}_{2_{r-}} \\ 0 & -I & I & 0 & \boldsymbol{C}_{2_r} \\ & 0 & 0 & & \boldsymbol{C}_{2_{r+}} \end{array}\right] \begin{bmatrix} \tilde{\boldsymbol{g}}^{1'} & 0 \\ 0 & \tilde{\boldsymbol{g}}^2 \end{bmatrix} \begin{bmatrix} \boldsymbol{\lambda}^1_{i-} \\ \lambda_q \\ \lambda_s \\ \boldsymbol{\lambda}^1_{i+} \\ \boldsymbol{\lambda}^2 \end{bmatrix} = 0$$

Applying the relationship in Eq. (9) yields

$$\boldsymbol{C}\begin{bmatrix} \tilde{\boldsymbol{g}}^1_{i-} & 0 & 0 & 0 & 0 \\ 0 & \boldsymbol{g}_q & 0 & 0 & 0 \\ 0 & 0 & \boldsymbol{g}_s & 0 & 0 \\ 0 & 0 & 0 & \tilde{\boldsymbol{g}}^1_{i+} & 0 \\ 0 & 0 & 0 & 0 & \tilde{\boldsymbol{g}}_2 \end{bmatrix}\begin{bmatrix} \boldsymbol{\lambda}^1_{i-} \\ \lambda_i \|\boldsymbol{g}_i\|_2/\|\boldsymbol{g}_q\|_2 \\ \lambda_i \|\boldsymbol{g}_i\|_2/\|\boldsymbol{g}_s\|_2 \\ \boldsymbol{\lambda}^1_{i+} \\ \boldsymbol{\lambda}^2 \end{bmatrix} = 0$$

This and the result of condition 2,

$$\boldsymbol{g}_q/\|\boldsymbol{g}_q\|_2 = \boldsymbol{g}_s/\|\boldsymbol{g}_s\|_2 = \boldsymbol{g}_i/\|\boldsymbol{g}_i\|_2$$

gives

$$\boldsymbol{C}\begin{bmatrix} \tilde{\boldsymbol{g}}^1_{i-} & 0 & 0 & 0 & 0 \\ 0 & \boldsymbol{g}_i & 0 & 0 & 0 \\ 0 & 0 & \boldsymbol{g}_i & 0 & 0 \\ 0 & 0 & 0 & \tilde{\boldsymbol{g}}^1_{i+} & 0 \\ 0 & 0 & 0 & 0 & \tilde{\boldsymbol{g}}_2 \end{bmatrix}\begin{bmatrix} \boldsymbol{\lambda}^1_{i-} \\ \lambda_i \\ \lambda_i \\ \boldsymbol{\lambda}^1_{i+} \\ \boldsymbol{\lambda}^2 \end{bmatrix}$$

$$= \boldsymbol{C}\begin{bmatrix} \tilde{\boldsymbol{g}}^1_{i-} & 0 & 0 & 0 \\ 0 & \boldsymbol{g}_i & 0 & 0 \\ 0 & \boldsymbol{g}_i & 0 & 0 \\ 0 & 0 & \tilde{\boldsymbol{g}}^1_{i+} & 0 \\ 0 & 0 & 0 & \tilde{\boldsymbol{g}}^2 \end{bmatrix}\begin{bmatrix} \boldsymbol{\lambda}^1_{i-} \\ \lambda_i \\ \boldsymbol{\lambda}^1_{i+} \\ \boldsymbol{\lambda}^2 \end{bmatrix} = 0$$

Finally, simple manipulations reduce these equilibrium conditions to

$$\left[\begin{array}{c|c|c|c} & 0 & & \\ & \boldsymbol{I} & \leftarrow \nu_j & \\ \boldsymbol{C}^{1_{i-}} & 0 & \boldsymbol{C}^{1_{i+}} & 0 \\ & -\boldsymbol{I} & \leftarrow \nu_k & \\ & 0 & & \\ \hdashline & 0 & & \boldsymbol{C}_{2_{r-}} \\ 0 & 0 & 0 & \boldsymbol{C}_{2_r} \\ & 0 & & \boldsymbol{C}_{2_{r+}} \end{array}\right]\begin{bmatrix} \tilde{\boldsymbol{g}}^1_{i-} & 0 & 0 & 0 \\ 0 & \boldsymbol{g}_i & 0 & 0 \\ 0 & 0 & \tilde{\boldsymbol{g}}^1_{i+} & 0 \\ 0 & 0 & 0 & \tilde{\boldsymbol{g}}^2 \end{bmatrix}\begin{bmatrix} \boldsymbol{\lambda}^1_{i-} \\ \lambda_i \\ \boldsymbol{\lambda}^1_{i+} \\ \boldsymbol{\lambda}^2 \end{bmatrix} = 0$$

which has the identical form as Eq. (10). This proves that attaching nodes to elements does not violate equilibrium if it is performed in concordance with conditions 2 of the theorem.

We omit the proof of the obvious fact that the element superposition does not violate equilibrium of the structure if it is performed in concordance with condition 3. □

Theorem 1 indicates that the fact that a tensegrity structure represents a composition of several tensegrity structures is related to the dimension of its prestress cone.[22]

Result 1: The structure that is the composition of n_c equilibrium tensegrity structures, each of which has n_{pm_i}, $i = 1 \ldots n_c$, prestress modes, has at least $n_{pm} = \sum n_{pm_i}$ prestress modes.

The composition of n_c component structures that can be classified in n_m groups of identical structures, called the modules, will be called the n_m-hedral modular tensegrity structure. If the structure has only one module, then the module will be called the unit and the structure monohedral.

Observe that the tensegrity plates[6] in Fig. 2 represent monohedral modular tensegrity structures, and they are composed of identical one-stage shell-class tensegrity units. The plates depicted are composed of four- and six-bar tensegrity units. The specific symmetry of these structures is caused by the particular relative positions of the units in the plates.

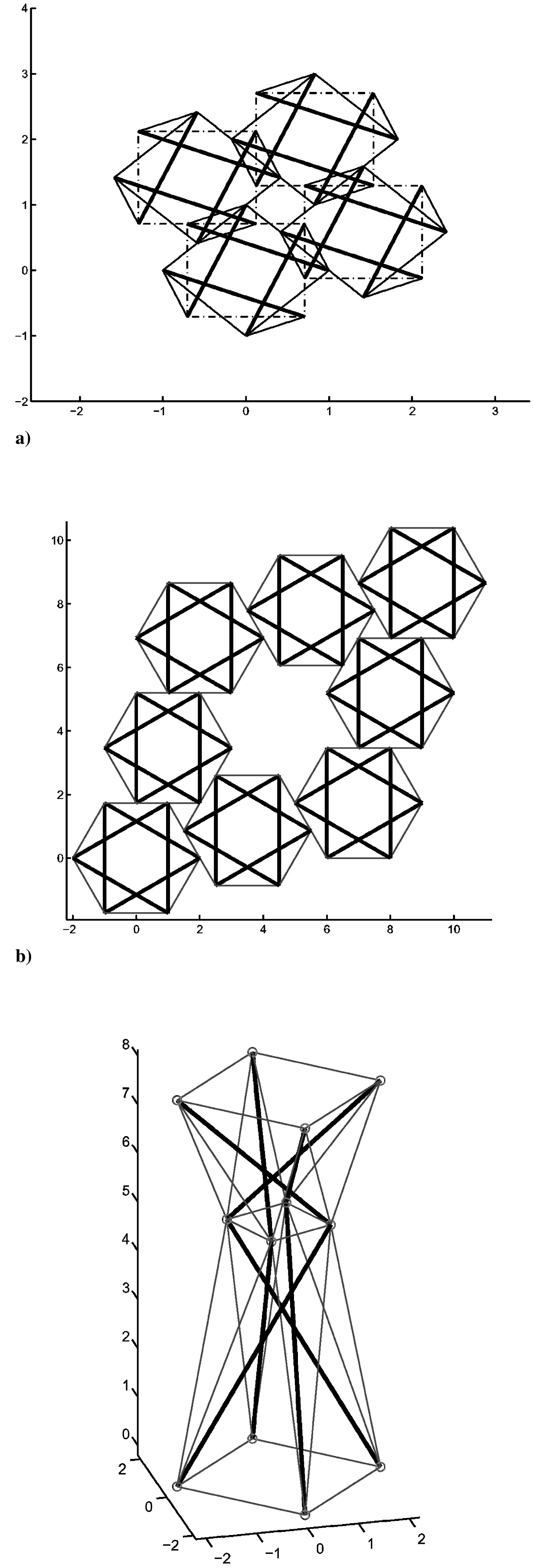

Fig. 2 Examples of modular tensegrities: tensegrity plates (panels a and b) made of four- and six-bar units and tensegrity tower (panel c) composed of four-bar modules.

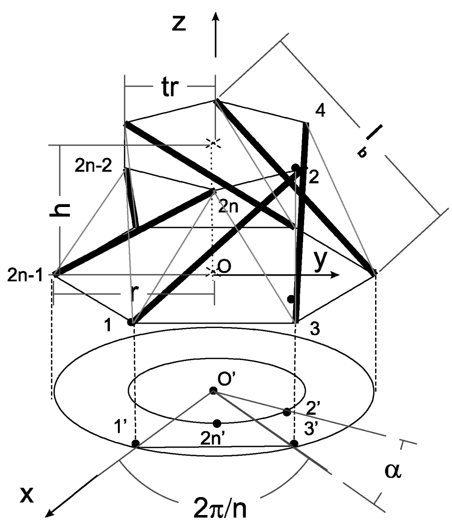

Fig. 3a Geometry of the symmetric one-stage shell-class module defining its geometric parameters.

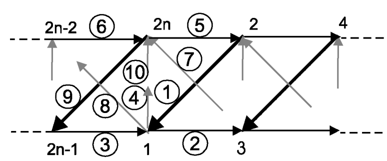

Fig. 3b Node and element numbering for different connectivity schemes.

IV. Geometry and Equilibrium Analysis of One-Stage Shell-Class Tensegrity Module

In the sequel geometry and equilibrium conditions are investigated for the tensegrity structure that serves as a module in larger tensegrity structures.

A. Module Geometry

We analyze a n-bar shell-class[21] tensegrity in the configuration that admits n-fold rotational symmetry C_n about z axis as the nodal symmetry. Its nodal positions can be expressed in terms of geometric parameters[22] l_b, r, α, t, which are depicted in Fig. 3, and the constant matrix $\mathcal{R}$ that reflects symmetry of the structure. The nodal vector of the structure $\boldsymbol{p} \in \mathbb{R}_3^{2n}$ can be related to these parameters in the following compact form[22]:

$$\boldsymbol{p} = \mathcal{R}\underline{\boldsymbol{p}}, \qquad \underline{\boldsymbol{p}} = \underline{\boldsymbol{p}}(n, l_b, r, \alpha, t) = \begin{bmatrix} \boldsymbol{p}_1(n, l_b, r, \alpha, t) \\ \boldsymbol{p}_{2n}(n, l_b, r, \alpha, t) \end{bmatrix} \tag{14}$$

Define matrix R of the rotation about the z axis:

$$R(x) = \begin{bmatrix} \cos x & \sin x & 0 \\ -\sin x & \cos x & 0 \\ 0 & 0 & 1 \end{bmatrix} \tag{15}$$

The nodal parameterization (14) takes the following form:

$$\begin{aligned} \boldsymbol{p}_1 &= [r \quad 0 \quad 0]^T, & \boldsymbol{p}_3 &= R(2\pi/n)\boldsymbol{p}_1 \\ \boldsymbol{p}_{2n-1} &= R^{-1}(2\pi/n)\boldsymbol{p}_1 & \boldsymbol{p}_{2n} &= R(\alpha)[tr \quad 0 \quad h]^T \\ \boldsymbol{p}_2 &= R(2\pi/n)\boldsymbol{p}_{2n}, & \boldsymbol{p}_{2n-2} &= R^{-1}(2\pi/n)\boldsymbol{p}_{2n} \end{aligned} \tag{16}$$

The requirement that the height h of the structure be a positive real number yields the following definition of the feasible set for the geometric variables:

$$h = \sqrt{l_b^2 - r^2 - r^2t^2 + 2r^2t\cos(2\pi/n + \alpha)} \tag{17}$$

$$0 < r < l_b \big/ [1 + t^2 - 2t\cos(2\pi/n + \alpha)], \qquad 0 < t, \quad 0 < l_b \tag{18}$$

B. Equilibrium of One-Stage Shell-Class Tensegrity Module

All configurations that admit the given nodal symmetry are parameterized by Eqs. (16), regardless of equilibrium conditions being satisfied. One must solve Eqs. (7) to find the subset of these symmetric configurations that yield equilibrium tensegrity structures. Because of the element symmetry, equilibrium equations in Eqs. (7) can be reduced to the balance of the forces equations at only two representative nodes ν_1 and ν_{2n}. The element vectors appearing in the equilibrium equations at nodes ν_1 and ν_{2n} are computed as

$$\boldsymbol{g}_1 = \boldsymbol{p}_1 - \boldsymbol{p}_2, \qquad \boldsymbol{g}_2 = \boldsymbol{p}_3 - \boldsymbol{p}_1, \qquad \boldsymbol{g}_3 = \boldsymbol{p}_1 - \boldsymbol{p}_{2n-1}$$

$$\boldsymbol{g}_4 = R[-m(2\pi/n)]\boldsymbol{p}_{2n} - \boldsymbol{p}_1, \qquad \boldsymbol{g}_5 = \boldsymbol{p}_2 - \boldsymbol{p}_{2n}$$

$$\boldsymbol{g}_6 = \boldsymbol{p}_{2n} - \boldsymbol{p}_{2n-2}, \qquad \boldsymbol{g}_7 = \boldsymbol{p}_{2n} - R[q(2\pi/n)]\boldsymbol{p}_3$$

$$\boldsymbol{g}_8 = R[-q(2\pi/n)]\boldsymbol{p}_{2n-2} - \boldsymbol{p}_1, \qquad \boldsymbol{g}_9 = \boldsymbol{p}_{2n-1} - \boldsymbol{p}_{2n}$$

$$\boldsymbol{g}_{10} = \boldsymbol{p}_{2n} - R[m(2\pi/n)]\boldsymbol{p}_1$$

The set of equations defining the equilibrium configuration of the module becomes

$$\boldsymbol{g}_1\lambda_1 + \boldsymbol{g}_2\lambda_2 - \boldsymbol{g}_3\lambda_3 + \boldsymbol{g}_4\lambda_4 + \boldsymbol{g}_8\lambda_8 = 0$$

$$\boldsymbol{g}_5\lambda_5 - \boldsymbol{g}_6\lambda_6 - \boldsymbol{g}_7\lambda_7 - \boldsymbol{g}_9\lambda_9 - \boldsymbol{g}_{10}\lambda_{10} = 0$$

$$\lambda_i \geq 0$$

The element symmetry of the structure allows further reduction in the number of force density variables:

$$\lambda_9 = \lambda_1, \qquad \lambda_3 = \lambda_2, \qquad \lambda_6 = \lambda_5, \qquad \lambda_8 = \lambda_7, \qquad \lambda_{10} = \lambda_4 \tag{19}$$

If one defines matrices $\boldsymbol{D}, \boldsymbol{C}, \tilde{\boldsymbol{g}}, Q$ corresponding to the problem and casts the problem in the standard form (7), the equilibrium conditions reduce to the following compact form:

$$\boldsymbol{D}\boldsymbol{C}\tilde{\boldsymbol{g}}Q\underline{\lambda} = 0 \tag{20}$$

$$\underline{\lambda} = [\lambda_1 \quad \lambda_2 \quad \lambda_4 \quad \lambda_5 \quad \lambda_7]^T \tag{21}$$

$$\lambda_i \geq 0 \tag{22}$$

Hence, $\underline{\lambda}$ that solves Eq. (20) is computed as a vector in the null space of $\boldsymbol{D}\boldsymbol{C}\tilde{\boldsymbol{g}}Q$. Because the basis $\underline{\Lambda}$ of the null space of $\boldsymbol{D}\boldsymbol{C}\tilde{\boldsymbol{g}}Q$ is one dimensional, the solution $\underline{\lambda}$ is given by

$$\lambda_1 \geq 0 \tag{23}$$

$$\lambda_2 = \lambda_1 \frac{t\csc^2(\pi/n)\sin[(m+1)\pi/n]\sin[(q+2)\pi/n]}{2\cos[(m+q+1)\pi/n - \alpha]} \tag{24}$$

$$\lambda_5 = \lambda_1 \frac{\csc^2(\pi/n)\sin[(m+1)\pi/n]\sin[(q+2)\pi/n]}{2t\cos[(m+q+1)\pi/n - \alpha]} \tag{25}$$

$$m - q \neq 1 \tag{26}$$

$$\lambda_4 = \lambda_1 \frac{\cos(q\pi/n - \alpha)\sin[(q+2)\pi/n]}{\cos[(m+q+1)\pi/n - \alpha]\sin[(q-m+1)\pi/n]} \tag{27}$$

$$\lambda_7 = -\lambda_1 \frac{\cos[(1-m)\pi/n + \alpha]\sin[(1+m)\pi/n]}{\sin[(q-m+1)\pi/n]\cos[(m+q+1)\pi/n - \alpha]} \tag{28}$$

$$m - q = 1 \tag{29}$$

$$\lambda_4 = \lambda_1 \tag{30}$$

$$\lambda_7 = 0 \tag{31}$$

which can be written in a more compact form:

$$\underline{\lambda} = \underline{\Lambda}\lambda_1, \qquad \underline{\Lambda} = \underline{\Lambda}(n, \alpha, t, m, q) \tag{32}$$

The connectivity for which $m - q = 1$ corresponds to the case where the strings e_4 and e_{10} overlap, so that they can be substituted with a single string.

For a given number of bars n and string connectivity parameters m and q, the permissible α can be computed from the condition

$$\lambda_i \geq 0 \tag{33}$$

The solution to

$$\lambda_7 = 0, \qquad \lambda_4 = 0 \tag{34}$$

for α gives the values of angle α where λ_7 and λ_4 change their signs,

$$\alpha = \pi/2 + (m-1)(\pi/n), \qquad \alpha = \pi/2 + q\pi/n \tag{35}$$

Finally, it can be verified that the admissible α is defined as

$$\underline{\alpha} = \min[\pi/2 + q\pi/n, \pi/2 + (m-1)(\pi/n)] \tag{36}$$

$$\bar{\alpha} = \max[\pi/2 + q\pi/n, \pi/2 + (m-1)(\pi/n)] \tag{37}$$

$$\alpha \in [\underline{\alpha}, \bar{\alpha}] \tag{38}$$

Note that if the string e_4 and the string e_7 are both present in the structure, equilibrium geometry is not unique. That is, Eqs. (36–38) define the range of α that yields an equilibrium tensegrity geometry. In the case where either of these two different groups of strings is not present in the structure, the equilibrium geometry becomes unique, and it is defined by the corresponding limits of α. A more detailed analysis of the module equilibrium for several different connectivity cases and asymmetric distribution of the prestress is provided by Masic.[23]

Note that the basis Λ for the prestress cone $\mathcal{C}(\Lambda)$ depends only on the twist angle α and the truncation ratio parameter t. This is a result of the fact that all symmetric nodal configurations where these two parameters are kept constant are related through the tensegrity similarity transformations of the form $\boldsymbol{p}^2 = T(\boldsymbol{p}^1)$ with $\boldsymbol{p}_i^2 = A\boldsymbol{p}_i^1$. This geometric transformation does not alter the equilibrium of the structure and associated force density variables regardless of the choice for the constant matrix $A \in \mathbb{R}^{3\times 3}$ (Ref. 22). The relationship between geometry of any two tensegrity modules that share common n, r, α, and t, but different bar lengths $l_{b_1} \neq l_{b_2}$, has the form of a similarity transformation with

$$A = \begin{bmatrix} 1 & 0 & 0 \\ 0 & 1 & 0 \\ 0 & 0 & h_1/h_2 \end{bmatrix}$$

where h_1 and h_2 are computed from Eq. (17). In the view of this result, equilibrium analysis of the one-stage module represents a solution of equilibrium conditions for the elliptical module derived by a similarity transformation from the unit that admits C_n symmetry about the z axis.

V. Geometry and Equilibrium of Monohedral Modular Tensegrity Plates

By a simple observation, it has already been inferred that the tensegrity plates in Fig. 2 belong to the class of monohedral modular tensegrity structures. The shape of the modules (units) and their relative positions allow the whole plane of the plate to be filled with the identical units to compose a monohedral periodic infinite plate. The set $\mathbb{P}_\infty^c$ of geometrical centers $\boldsymbol{p}_i^c \in \mathbb{R}^3$ of the units of the infinite plate represents a lattice spanned by two linearly independent vectors $\boldsymbol{s}_1 \in \mathbb{R}^3$ and $\boldsymbol{s}_2 \in \mathbb{R}^3$ called lattice generators, so that $\boldsymbol{p}_i^c = a_i\boldsymbol{s}_1 + b_i\boldsymbol{s}_2,\ a_i, b_i \in Z$ (see Fig. 4). The only tensegrity plates of interest for this analysis are the ones that can be regarded as sections of the infinite periodic monohedral tensegrity plates that are composed of n-bar one-stage shell-class tensegrities units that admit C_n symmetry. In other words, the plate can be defined by the composition of the finite number of units of the infinite plate whose geometrical centers belong in the subset $\mathbb{P}^c \in \mathbb{P}_\infty^c$ of the associated infinite plate.

In the next section we analyze the relationship between the geometric parameters of the unit and the parameters of the associated lattice that enables composition of the units in the periodic plate.

A. Geometry of Four- and Six-Bar Unit Monohedral Modular Plates

We analyze relative positions of the units of the plates in Fig. 4. Let strings $e_{2'}$ and $e_{2''}$, $e_{6'}$ and $e_{6''}$ be formed after dividing strings e_2 and e_6 as the result of the composition of the two units as indicated in Fig. 4. In this analysis we compute only the overlap parameter γ. This parameter defines the lengths of the strings $e_{2'}$ and $e_{2''}$, which are generated by attaching nodes of a unit to elements of an adjacent unit, and it represents the ratio $\gamma = l_2/l_{2'}$. It is the only parameter of the overall plate geometry that appears in the formulation of our plate control algorithm. Masic[23] provides a more detailed analysis

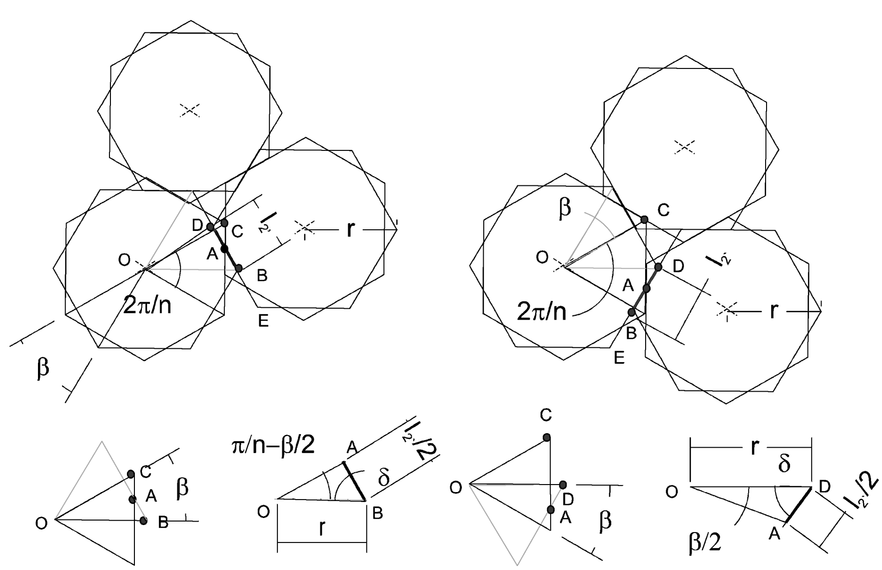

Fig. 4 Relative position of adjacent units in periodic tensegrity plates. Two different topologies can be generated by utilizing the same unit. Changing the lattice parameters yields the two distinct structures depicted at the left and right.

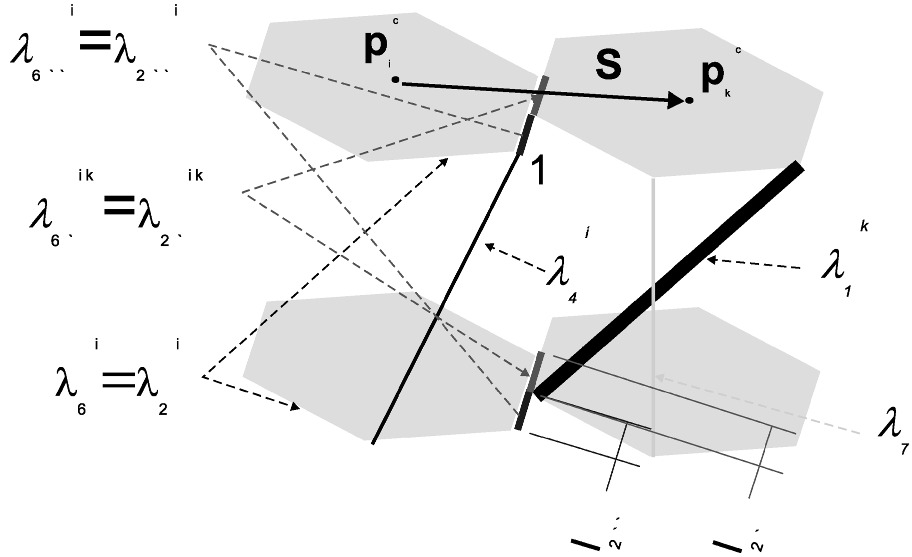

Fig. 5 Force distribution in the *n*-bar stable unit plate.

of different plate topologies. Define angle β as the angle between the projections of the top and bottom polygon of the unit onto $x-y$ plane. This angle is generally different from the angle α and is computed as

$$\beta = \mathrm{mod}[\alpha, (2\pi/n)] \tag{39}$$

where $\mathrm{mod}(x, y)$ is the remainder operator of the division x/y. Define angle δ as a half of the angle of a regular n-sided polygon that can be computed as

$$\delta = (\pi - 2\pi/n)/2 = \pi/2 - \pi/n \tag{40}$$

The overlap ratio γ for four- and six-bar units can be computed for both connectivity cases by computing the length of the element $e_{2'}$ connecting the nodes at D and B in Fig. 4. In the first connectivity case, for $\beta \neq 0$, length $l_{2'}$ of the string $e_{2'}$ is computed by applying the law of sines to triangle OAB:

$$\sin(\pi - \delta - \pi/n + \beta/2)/r = \sin(\pi/n - \beta/2)/(l'_2/2) \tag{41}$$

Substituting Eq. (40) into Eq. (41) and dividing length $l_{2'}$ by the total length l_2 of the string connecting nodes at D and E yields

$$\gamma = l_{2'}/\overline{DE} = l_{2'}/l_2 = 1 - \tan(\beta/2) \tag{42}$$

Similarly, it can be verified that in the second connectivity case the feasible overlap ratio satisfies

$$\gamma = l_{2'}/\overline{DE} = l_{2'}/l_2 = \csc(\pi/n)\sec(\pi/n - \beta/2)\sec(\beta/2) \tag{43}$$

Observe that when $\beta = 0$ the overlap ratio γ is not unique for both connectivity cases, and it can take values $\gamma \in [0, 1]$.

B. Equilibrium of Stable Unit Tensegrity Plates and Class-2 Tensegrity Towers

A monohedral modular tensegrity plate can be formed from its modules by a sequence of structure composition operations. All of n_m one-stage shell-class modules must share the same geometric parameters n, l_b, r, α, t in Eqs. (14) but not necessarily the same value for the force density λ_1 in Eqs. (23–31). The collection of these force densities for all of the modules parameterizes the prestress cone of the stable unit plate. Let the collection of force densities, $\lambda^i_1 \geq 0,\ i = 1, \ldots, n_m$, of the bars of the n_m modules be given. Let $\lambda^i_j = \lambda_j(\lambda^i_1)$ denote the solutions λ_j of Eqs. (23–31) and Eqs. (19) when $\lambda_1 = \lambda^j_1$. Let λ^{ik}_j denote the force densities of the elements introduced by the composition of the two adjacent units with centers $\boldsymbol{p}^c_i$ and $\boldsymbol{p}^c_k$ (Fig. 5). Equations (44–50) define equilibrium force densities for all elements in the plate:

$$\lambda^i_j = \lambda_j(\lambda^i_1), \qquad j = 1, 4, 5, \quad \text{or} \quad 7 \tag{44}$$

$$n = 4, 6 \tag{45}$$

$$\lambda^{ik}_j = \lambda_2\big(\lambda^i_1\big)\big/\gamma + \lambda_2\big(\lambda^k_1\big)\big/\gamma, \qquad j = 2', 6' \tag{46}$$

$$\lambda^i_j = \lambda_2\big(\lambda^i_1\big)\big/(1-\gamma), \qquad j = 2'', 6'' \tag{47}$$

$$n = 3 \tag{48}$$

$$\lambda^i_j = \lambda_2\big(\lambda^i_1\big)\big/\gamma, \qquad j = 2', 6' \tag{49}$$

$$\lambda^i_j = \lambda_2\big(\lambda^i_1\big)\big/(1-\gamma), \qquad j = 2'', 6'' \tag{50}$$

These equilibrium conditions are a direct consequence of the application of Theorem 1 to composition of equilibrium tensegrity units. Note that the plate need not be fully populated with modules, as shown in the center structure of Fig. 2. The class-1 tensegrity towers can be viewed as composition of n_m class-1 tensegrity modules. All of these modules have the same number of bars per stage and admit n-fold rotational symmetry C_n. The only constraint for n_m of these equilibrium tensegrity structure to be compatible for the composition operation is that the radii of the top and bottom of the two adjacent structures are the same. This enables the top nodes of one module to be attached to the bottom nodes of the adjacent module (see Fig. 6). For a given collection of n_m compatible equilibrium tensegrity modules, Theorem 1 guarantees that the series of $n_m - 1$ compositions yields an equilibrium class-2 tensegrity tower.

VI. Slowly Varying Nonlinear Systems and Open Loop-Control

A. Parameterization of Tensegrity Structure Nonlinear Dynamic Model

Several different nonlinear models of tensegrity structures have been derived.[20,21] What is common for all of them is that rest lengths of elastic elements are parameters of the model. The open-loop control strategy that is postulated to control reconfiguration of equilibrium tensegrity structures is a result of a well-known result from nonlinear control theory.

Proposition 1: Let a parameterized model of a nonlinear system be given in the state-space form

$$\frac{\mathrm{d}\boldsymbol{x}}{\mathrm{d}\tau} = f(\boldsymbol{x}, \delta), \qquad \boldsymbol{x} \in R^n \tag{51}$$

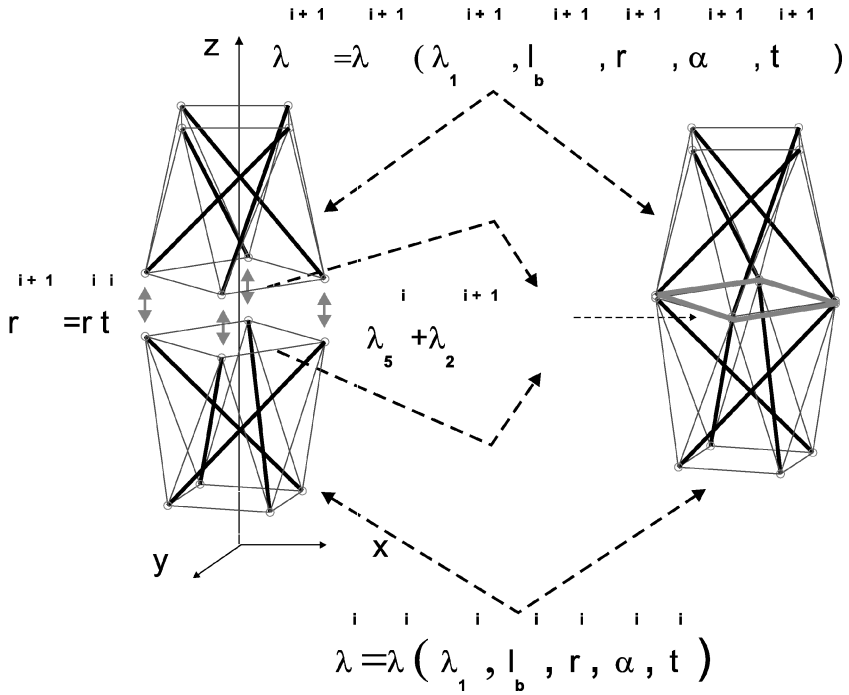

Fig. 6 Composition of tower modules.

where δ represents the set of parameters defining the model of the system. Let $\boldsymbol{g}(\delta)$ satisfying

$$0 = f[\boldsymbol{g}(\delta), \delta] \tag{52}$$

be an exponentially stable equilibrium manifold of the system. If a sufficiently slowly varying function $\delta = \delta(\tau)$ is defined, then trajectory $\boldsymbol{x}(\tau)$ of the system $\dot{\boldsymbol{x}} = f[\boldsymbol{x}, \delta(\tau)]$ tracks the equilibrium manifold $\boldsymbol{g}[\delta(\tau)]$.

Several references can be consulted for a more detailed analysis related to this topic.[24]

B. Equilibrium Rest-Lengths Parameterization

For a given equilibrium tensegrity structure $\Gamma = \{\mathbb{E}, \mathbb{P}, \Lambda\}$, depending on the material model used to build its elastic elements, rest lengths l_{0_i} of the elastic elements e_i are computed as

$$l_{0_i} = l_{0_i}(\lambda_i, l_i, z_i, y_i, a_i, \ldots) \tag{53}$$

where the meaning of the parameters $y_i, a_i, \ldots$ appearing in Eq. (53) depends on the material strain–stress relationship. In particular, for the linear elastic material model of elastic elements with the cross-section area a_i and Young's modulus y_i the force–strain relationship given by Hooke's law

$$f_i = \lambda_i l_i = z_i y_i a_i \big/ l_{0_i} \left(l_i - l_{0_i}\right)$$

results so that Eq. (53) has the following form:

$$l_{0_i} = \frac{z_i l_i y_i a_i}{l_i \lambda_i + z_i y_i a_i} \tag{54}$$

Note that the lengths l_i of all elements of the structure Γ depend only on the structure geometry $\mathbb{P}$ and connectivity $\mathbb{E}$. For the structures analyzed here, equilibria have been parameterized in terms of the set Ω of feasible geometry and force parameters:

$$\boldsymbol{p} = \boldsymbol{p}(n, \boldsymbol{l}_b, \boldsymbol{r}, \boldsymbol{\alpha}, \boldsymbol{t}, \gamma)$$

$$\boldsymbol{\lambda} = \Lambda \underline{\underline{\boldsymbol{\lambda}}}, \qquad \Lambda = \Lambda(n, \boldsymbol{l}_b, \boldsymbol{r}, \boldsymbol{\alpha}, \boldsymbol{t}, \gamma)$$

$$\underline{\underline{\boldsymbol{\lambda}}}, \boldsymbol{l}_b, \boldsymbol{r}, \boldsymbol{\alpha}, \boldsymbol{t}, \gamma \in \Omega \tag{55}$$

so that the equilibrium rest lengths are defined as

$$\boldsymbol{l}_0 = \boldsymbol{l}_0(\underline{\underline{\boldsymbol{\lambda}}}, \boldsymbol{l}_b, \boldsymbol{r}, \boldsymbol{\alpha}, \boldsymbol{t}, \gamma) \tag{56}$$

once the material and cross sections have been assigned to all elements of the structure Γ.

Recall that the rest lengths l_0 of the elastic members serve as the parameters δ of the nonlinear dynamic model of the system (51), so that using Eqs. (51) and (56) yields the parameterized structure model

$$\dot{\boldsymbol{x}} = f[\boldsymbol{x}, \boldsymbol{l}_0(\underline{\underline{\boldsymbol{\lambda}}}, \boldsymbol{l}_b, \boldsymbol{r}, \boldsymbol{\alpha}, \boldsymbol{t}, \gamma)] = f(\boldsymbol{x}, \underline{\underline{\boldsymbol{\lambda}}}, \boldsymbol{l}_b, \boldsymbol{r}, \boldsymbol{\alpha}, \boldsymbol{t}, \gamma) \tag{57}$$

Proposition 1 suggests that the system (57) tracks the equilibrium configuration:

$$\boldsymbol{p}(\tau) = \boldsymbol{p}[\boldsymbol{l}_b, \boldsymbol{r}(\tau), \boldsymbol{\alpha}(\tau), \boldsymbol{t}(\tau), \gamma(\tau)]$$

if one defines the sufficiently slowly varying functions

$$\underline{\underline{\boldsymbol{\lambda}}}(\tau), \boldsymbol{r}(\tau), \boldsymbol{\alpha}(\tau), \boldsymbol{t}(\tau), \gamma(\tau) \in \Omega$$

that define the desired configuration $\boldsymbol{p}(\tau)$ and the force densities $\boldsymbol{\lambda}(\tau)$ at every time instance τ.

Assume that all bar elements are rigid, with fixed lengths $\boldsymbol{l}_b$ as it is postulated in several models.[21] Then the only parameters of the desired geometry of the system that can be time dependent are $\underline{\underline{\boldsymbol{\lambda}}}(\tau), \boldsymbol{r}(\tau), \boldsymbol{\alpha}(\tau)$, and $\boldsymbol{t}(\tau)$, and additionally $\gamma(\tau)$ for some stable unit plates, so that the string elements rest-length open-loop control becomes

$$l_{0_i}(\tau) = l_{0_i}[\underline{\underline{\boldsymbol{\lambda}}}(\tau), \boldsymbol{r}(\tau), \boldsymbol{\alpha}(\tau), \boldsymbol{t}(\tau), \gamma(\tau)], \qquad e_i \in \mathbb{E}_s \tag{58}$$

VII. Examples

A. Plate Deployment

The control objective is to deploy the 8×8 modules six-bar unit plate with bar lengths $l_b = 2$. To define the control law (58), a monotonically increasing function $r(\tau)$ on the interval $(0, T)$ is defined. Any monotonically increasing $r(\tau)$ on the interval $(0, T)$ drives the plate from the stowed configuration with $r(0)$ at $\tau = 0$ to the deployed configuration with $r = r(T) > r(0)$ at $\tau = T$. In the same fashion a monotonically decreasing $r(\tau)$ should be defined to stow

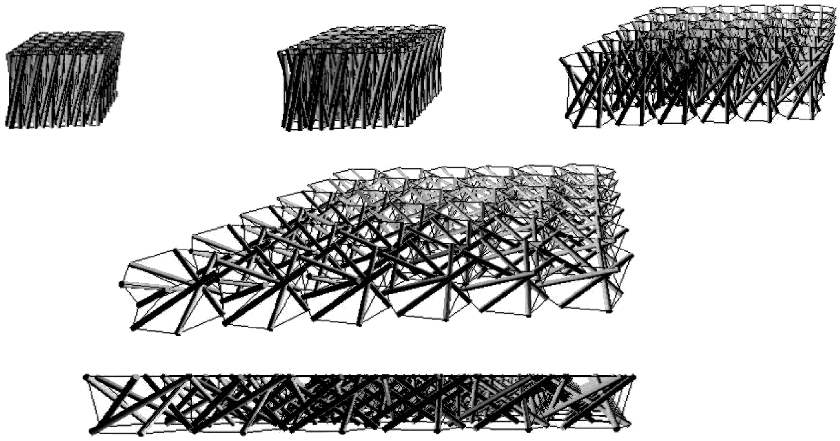

Fig. 7 Open-loop controlled deployment of a six-bar unit plate.

the structure back. The desired geometry parameter functions in Eq. (58) are defined as follows:

$$r(\tau) = 0.2 + 0.04\tau, \quad \alpha(\tau) = \pi/3, \quad t = 1, \quad \gamma(\tau) = 0.2 + 0.02\tau$$
$$0 < \tau \leq 20$$
$$r(\tau) = 1, \quad \alpha(\tau) = \pi/3, \quad t = 1, \quad \gamma(\tau) = 0.6$$
$$20 < \tau \leq 30$$

Bar force densities $\lambda_1^i(\tau)$ of all of the 64 modules are set to be the same throughout the deployment, so that $\underline{\underline{\lambda}}_i(\tau) = \lambda_1^i(\tau) = \lambda_1(\tau)$ and

$$\lambda_1(\tau) = 1, \qquad 0 < \tau \leq 20$$
$$\lambda_1(\tau) = 1 - 0.02(\tau - 20), \qquad 20 < \tau \leq 25$$
$$\lambda_1(\tau) = 0.9, \qquad 25 < \tau \leq 30$$

Simulation results are depicted in Fig. 7. The ratio between the areas of the plate in the final and initial configuration is approximately 25.

B. Tower Deployment

The control objective in this example is to deploy the class-2 tensegrity tower composed of four one-stage four-bar modules with bar lengths $l_b = 6$. To define the deployment control law (58), a monotonically decreasing function $r(\tau)$ on the interval $(0, T)$ is defined. The desired geometry parameter functions in Eq. (58) are defined as follows:

$$r(\tau) = 3.2 - 0.05\tau, \qquad \alpha(\tau) = \pi/4, \qquad t = 1$$
$$0 < \tau \leq 10$$
$$r(\tau) = 3.2 - 0.05\tau, \qquad \alpha(\tau) = \pi/4 + 0.03(10 - \tau)(\pi/4)$$
$$t = 1, \qquad 10 < \tau \leq 25$$
$$r(\tau) = 1.95, \quad \alpha(\tau) = 1.45(\pi/4), \qquad t = 1, \qquad 25 < \tau \leq 30$$

Unlike the geometric parameters that are common for all of the modules, force densities $\lambda_1^i(\tau)$ are not. They are set to be constant throughout the deployment, so that $\underline{\underline{\lambda}}(\tau) = [\lambda_1^1(\tau) \;\; \lambda_1^2(\tau) \;\; \lambda_3^2(\tau) \;\; \lambda_4^2(\tau)]^T$, with

$$\underline{\underline{\lambda}}(\tau) = [1 \quad 2 \quad 2 \quad 1], \qquad 0 < \tau \leq 30$$

Masic[23] provides the closed form of the string rest-length control. Simulation results are depicted in Fig. 8. The ratio between the initial and final height of the tower is approximately 4.5.

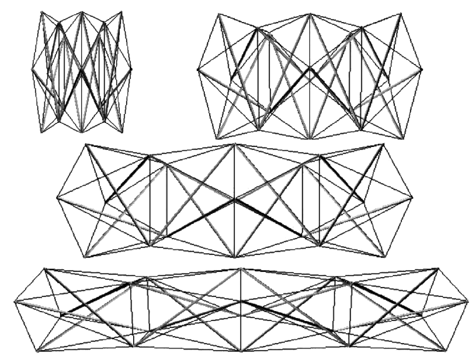

Fig. 8 Deployment of a class-1 tensegrity tower.

VIII. Conclusions

This paper analyzes properties of a special class of tensegrity structures called modular tensegrity structures. Particular symmetry of these structures is identified and implemented in a systematic way to simplify their equilibrium analysis. The set of structure composition rules are defined for analysis and syntheses of this class of structures. These rules show that the equilibrium of periodic modular tensegrity structures can be parameterized in terms of very few meaningful geometric and force parameters. Applications of these rules to several tensegrity structures in this paper provide equilibrium parametrizations for structures of arbitrary sizes.

The highly nonlinear nature of tensegrity structure models and the nonautonomous character of tracking control problems make the general tensegrity reconfiguration control a very difficult problem. Adding different performance requirements would make it even more difficult. Hence, we offer this open-loop control result as a solution for the tracking control problems associated with a wide class of tensegrity reconfiguration strategies.

The analysis of the structures in this paper identified a convenient set of parameters to characterize their equilibria and the set of feasible values for these parameters. We also identified the parameters useful for control in the open-loop control law. Nonuniqueness of the possible choices for these parameters enables additional optimization criteria in the study of optimal structural and control performances.

References

[1] Snelson, K., "Continuous Tension, Discontinuous Compression Structures," U.S. Patent 3,169,611, 16 Feb. 1965.

[2] Fuller, R. B., "Tensile-Integrity Structures," U.S. Patent, 3,063,521, Nov. 1962.

[3] Calladine, C., "Buckminster Fuller's Tensegrity Structures and Clerk Maxwell's Rules for the Construction of Stiff Frames," *International Journal of Solids and Structures*, Vol. 14, No. 2, 1978, pp. 161–172.

[4]Pellegrino, S., and Calladine, C., "Matrix Analysis of Statistically and Kinematically Indeterminate Frameworks," *International Journal of Solids and Structures*, Vol. 22, No. 4, 1986, pp. 409–428.

[5]Motro, R., "Tensegrity Systems: The State of the Art," *International Journal of Space Structures,* Vol. 7, No. 2, 1992, pp. 75–83.

[6]Hanaor, A., "Double-Layer Tensegrity Grids—Static Load Response. 1. Analytical Study," *Journal of Structural Engineering*, Vol. 117, No. 6, 1991, pp. 1660–1674.

[7]Connelly, R., and Whiteley, W., "Second Order Rigidity and Prestress Stability for Tensegrity Frameworks," *SIAM Journal of Discrete Mathematics*, Vol. 9, No. 3, 1996, pp. 453–491.

[8]Murakami, H., and Nishimura, Y., "Static and Dynamic Characterization of Regular Truncated Icosahedral and Dodecahedral Tensegrity Modules," *International Journal of Solids and Structures*, Vol. 38, Nos. 50–51, 2001, pp. 9359–9381.

[9]Feste, E., and Shea, K., Domer, B., and Smith, I., "Adjustable Tensegrity Structures," *Journal of Structural Engineering*, Vol. 129, No. 4, 2003, pp. 515–526.

[10]Tibert, A. G., and Pellegrino, S., "Deployable Tensegrity Masts," *Proceedings of the 44th AIAA/ASME/ASCE/AHS/ASC Structures, Structural Dynamics and Material Conference end Exhibit* [CD-ROM], AIAA, Reston, VA, 2003.

[11]Sultan, C., and Skelton, R., "Force and Torque Smart Tensegrity Sensor," *Proceedings of the 5th Annual Symposium or Smart Structures and Materials*, Vol. 3323, edited by V. V. Varadan, International Society for Optical Engineering, Bellingham, WA, 1998, pp. 357–368.

[12]Sultan, C., and Skelton, R., "Tendon Control Deployment of Tensegrity Structures," *Proceedings of the 5th Annual Symposium on Smart Structures and Materials*, Vol. 3323, edited by V. V. Varadan, International Society for Optical Engineering, Bellingham, WA, 1998, pp. 455–466.

[13]Sultan, C., Corless, M., and Skelton, R., "Nonlinear Robust Tracking Control of a Tensegrity Motion Simulator," *Proceedings of Smart Strutures and Materials Conference*, Vol. 3365, edited by M. K. Masten and L. A. Stockum, International Society for Optical Engineering, Bellingham, WA, 1998, pp. 179–190.

[14]Sultan, C., Corless, M., and Skelton, R., "Tensegrity Flight Simulator," *Journal of Guidance, Control, and Dynamics,* Vol. 23, No. 6, 2000,pp. 1055–1064.

[15]Masic, M., and Skelton, R. E., "Deployable Plates Made from Stable-Element Class 1 Tensegrity," *Proceedings of the 9th Smart Structures and Materials Conference*, Vol. 4698, edited by A. R. McGovan, Internatinal Society for Optical Engineering, Bellingham, WA, 2002, pp. 220–230.

[16]Sultan, C., Corless, M., and Skelton, R. E., "Symmetric Reconfiguration of Tensegrity Structures," *International Journal of Solids and Structures*, Vol. 39, No. 8, 2002, pp. 2215–2234.

[17]Sultan, C., Corless, M., and Skelton, R. E., "Deployment of Tensegrity Structures," *International Journal of Solids and Structures*, Vol. 40, No. 18, 2003, pp. 4637–4657.

[18]Sultan, C., and Skelton, R., "Integrated Design of Controllable Tensegrity Structures," *Proceedings of the ASME International Congress and Exposition*, Vol. 54, edited by D. Brei and J. Sirkis, American Society of Mechanical Engineers, New York, 1997, pp. 27–37.

[19]Kanchanasaratool, N., and Williamson, D., "Modelling and Control of Class NSP Tensegrity Structures," *International Journal of Control*, Vol. 75, No. 2, 2002, pp. 123–139.

[20]Murakami, H., "Static and Dynamic Analysis of Tensegrity Strutures. Part 1. Nonlinear Equations of Motion," *International Journal of Solids and Structures*, Vol. 38, No. 20, 2001, pp. 3599–3613.

[21]Skelton, R. E., Pinaud, J., and Mingori, D. L., "Dynamics of the Shell-Class of Tensegrity Structures," *Journal of the Franklin Institute*, Vol. 2–3, No. 338, 2001, pp. 255–320.

[22]Masic, M., Skelton, R. E., and Gill, P., "Algebraic Tensegrity Form-Finding," *International Journal of Solids and Structures* (submitted for publication).

[23]Masic, M., "Design, Optimization, and Control of Tensegrity Structures," Ph. D. Dissertation, Dept. of Mechanical and Aerospace Engineering, Univ. of California, La Jolla, CA.

[24]Khalil, H., *Nonlinear Systems*, 3rd ed., Preantice–Hall, Upper Saddle River, NJ, 2002, Chap. 9, pp. 365–372.